Machine Learning applied to fiber-fed focal plane wavefront sensors: a proposal for a comprehensive study

B. Di Francesco*[a], G. Di Rico [a], S. Di Frischia [a], M. Dolci [a], I. Di Antonio[a]

[a] INAF - Osservatorio Astronomico d'Abruzzo, Via Mentore Maggini, 64100 Teramo, Italy
*benedetta.difrancesco@inaf.it, phone: +39 0861439739

ABSTRACT

This research proposal aims to analyze the capabilities of Machine Learning to reconstruct the input features of an aberrated wavefront transmitted through an optical fiber, in view of focal plane wavefront sensing applications in ground-based telescopes. Future astronomical instrumentation, in fact, is increasingly moving towards photonic waveguides to carry information and fulfill stringent requirements for data acquisition and sensing.
Recent studies have provided insight into the generation of phase distortion on light propagation through fibers. Furthermore, Machine Learning based reconstruction methods, as applied to multimode and multicore fibers, have already demonstrated their potential in specialized medical fields. Building upon this knowledge, our objective is to study the feasibility of employing similar techniques for the development of astronomical instrumentation, thereby expanding the horizons of astrophotonics applications.

Keywords: optical fibers, wavefront sensing, adaptive optics, machine learning, neural networks, photonics

1. INTRODUCTION

Optical fibers are nowadays implemented in a wide range of applications due to their capacity to carry light through confined waveguides. Besides the use in telecommunications and information transmission [1,2], they have been largely involved as sensors for micro-vibrations, temperature, and pressure [3,4] as well as probes for endoscopy, ophthalmology, and bio-imaging [5,6].
Since 1970, optical fibers have been used in astronomical instrumentations, specifically for Multi-Object Spectroscopy (MOS) and Integral Field Spectroscopy (IFS), where the possibility of picking up the signal at the telescope focal plane and carrying it in a stable environment for further analysis, makes them suitable for these specific cases. Besides this, they found applications in high-precision radial-velocity work, interferometry, and photometry as auto-guider probes [7].
With the upcoming era of Extremely Large Telescope (ELT) instrumentations (ELT-MOSAIC, ELT-ANDES, GMT-MANIFEST etc.), they will play a decisive role, giving rise to a combination of photonics technologies in current Adaptive Optics (AO) devices.
New fiber-based Focal Plane Wavefront Sensors (FP-WFS) offer an example of this. They are aimed to overcome AO limitations due to Non-Common Path Aberrations (NCPA) [8] between the sensing and the scientific optical path or due to the Low Wind Effect (LWE) [9] inside the telescope dome. Recent works [10,11] highlighted the potentiality of a device called Photonic Lantern (PL) as Wavefront Sensor (WFS) at the focal plane of telescopes. The PL serves as a low-loss optical waveguide, linking a Multimode (MM) input core and a Multicore (MC) output, comprising a variable number of single-mode cores. This device was successfully implemented to simultaneously measure aberrations at the telescope focal plane through the analysis of the output Point Spread Function (PSF). In fact, the desired wavefront information can be determined by simply measuring the intensity of each single-mode output. The first PL probes involved a relatively small number of output cores, allowing for the identification of primarily low-order aberrations

from the output intensity pattern. Further advancements were made by augmenting the count of multicore outputs, providing the opportunity to investigate high-order terms and integrate deep learning into analysis. In fact, when supported by Machine Learning (ML) and Neural Networks (NN), the system acquires the ability to learn the mapping relationship between image distortions and wavefront aberrations. Moreover, one of NN key advantages is the ability to perform this mapping virtually with zero latency, meeting the demands of real-time control in a closed-loop setting. Consequently, in the field of Adaptive Optics, it demonstrates to be extremely suitable for the reconstruction and compensation of the distorted wavefront.

Building upon these comprehensive studies and prior research, our investigation starts by exploiting the transmission of an aberrated wavefront through Multimode Fibers (MMF), closely examining the propagation effects with the aid of Machine Learning. In contrast to PL, MMFs are widespread and cheaper tools with high transmission capabilities but no strict limitations on the number of modes excited. This is a feature that will be kept under control with awareness.

Nevertheless, in [12], MMFs have been used as major characters for endoscopic applications, demonstrating that multimode fibers can be more than just imaging devices and underlining their power for microsurgical applications through wavefront shaping. In addition, for more customized requirements, a trained deep neural network model proved to successfully recover the information delivered by MMF reducing complexity in computation.

Besides the known limitations of MMFs for what concerns mainly focal ratio degradation and modal noise, the main idea is to propose a similar investigation in astronomical applications and instrumentations.

2. BACKGROUND

Multimode fibers are able to support multiple transverse guided modes, whose number is determined by the working wavelength, the core diameter, and the refractive index profile.

Due to different propagation constants of the fiber modes, the local information transported by each mode messes up, forming a pattern at the fiber output that has a random intensity distribution. This pattern is called *speckle* and it is the result of the interference among the fiber modes emerging from the fiber. Despite this, the coupled information is not totally lost along the propagation, and it can be recovered. Different optical techniques have been proposed for this objective: analog phase conjugation, digital iterative methods, digital phase conjugation, and transmission matrix recovering by digital holography.

According to this, supposing not to bend or stress the MMF, when a signal is sent through the fiber, it is possible to reconstruct the input from the output, exploiting the effects of modes combination inside. The same principle applies to an aberrated wavefront because the degree of excitation of the modes propagating contains amplitude and phase information of the input itself.

Besides the previously listed methods, ML is a good candidate to avoid heavy computation and gain fast reconstruction. It was the basic idea applied to studies on reconstruction for MMF imaging probes (Figure 1).

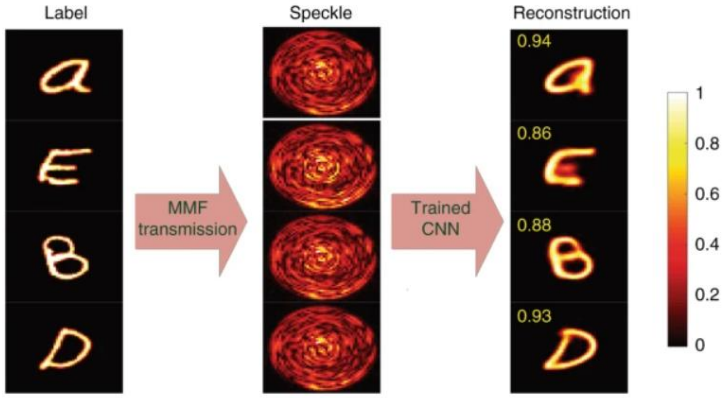

Figure 1. Example of imaging transmission and reconstruction [13] through MMF

In [13], a Latin alphabet letter from the MNIST database was first imaged onto a Spatial Light Modulator (SLM) and then focused on a multimode fiber facet. The output speckle was then recorded, and, through careful training of a deep

neural network, it was possible to determine with high accuracy the exact letter sent, even if the combination of modes scattered the initial information.
For our purpose, instead of sending a given letter or sign through the fiber, we want to analyze the effect of input-controlled turbulence on the output.
In fact, for our simulations, we were inspired by a work in the field of Free-Space Optical Communication (FSOC) [15], which analyses the effect of atmospheric turbulence on propagating light. In this specific case, a tradeoff between large core size fiber for coupling and high-capacity device was found in the use of Few Mode Fiber (FMF).

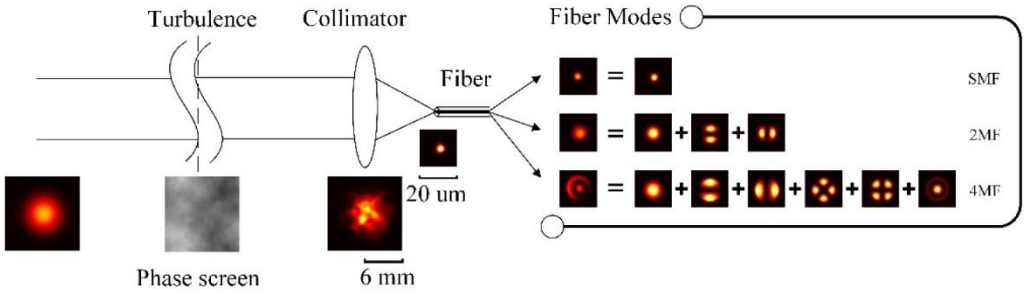

Figure 2. Experimental setup in [15] with FMF to study the effect of fiber propagation for a distorted beam

The beam is distorted by a phase modulator (SLM) which simulates a typical atmospheric turbulence, and the output intensity distribution is studied. Figure 3 shows the effect of aberrations for increasing values of atmospheric degradation as a function of D, the diameter of transmitting beams, and the Fried parameter r_0.

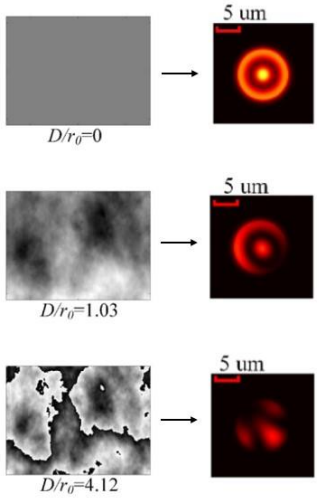

Figure 3. Effect of increasing atmospheric turbulence (on the left) on the output of a 4 modes FMF (on the right) [15]

Our work development is structured as follows: we begin by inducing an input aberration on one mode of the MMF, similar to the approach in [15]. However, in our case, aberrations are not defined by parameters D and r_0, but by a Zernike Polynomial. We then analyze the effect on the fiber output and, leveraging what was done in [13], try to define an input-output mapping of the system using ML.

3. METHODS AND SIMULATIONS

In the previous section, the potentiality of neural networks on fiber imaging as well as the possibility of studying the influence of aberrations on fiber output have been discussed.
The first step is to determine the feasibility of applying machine learning to the proposed problem. Subsequently, with a focus on ground-based telescope applications, we aim to assess the viability of the method itself.
This entails dedicating the initial part of the research to thoroughly exploring the output signal generated by a known input. During this phase, we must consider specific characteristics of the fiber:

1) length
2) core diameter
3) numerical aperture

Furthermore, we must take into account features related to the injected light (wavelength range, polarization state) and input geometry, such as the angle of incidence of the ray. Given the fiber's high sensitivity to environmental changes, it is crucial in this phase to study the effects of possible bending and mechanical strain.
To gain insight into fiber behavior, some simulations were carried out in an open-source simulation toolbox in Matlab [16], able to model a propagating electric field through a wide variety of optical fiber geometries.
It is important to emphasize that the following content comprises a sequence of tests and considerations that support the necessity for an extensive investigation into the propagation of an aberrated signal within a photonic medium. This underscores the significance of the parameters provided for the characterization of the input light and the optical fiber geometry. These parameters, specifically, will serve as guiding principles in the development of an optical bench intended for laboratory fiber testing.
To perform the simulations, we start with an initial field U_i, having a typical LP11 mode profile with a known intensity distribution. The superposition of an aberration on the initial field is carried on modifying U_i by introducing an additional phase term represented by Zernike polynomial [14]:

$$U = U_i e^{j\pi b Z_{nm}}$$

Where n and m are respectively the azimuthal and radial order of the polynomial Z_{nm}, and b is the corresponding Zernike coefficient, which represents the strength of the phase variation imposed.
In Figure 4, the input field intensity, without any aberration, is sketched for λ=800 nm, fiber Numerical Aperture (NA) equal to 0.24, and core diameter a = 100 um.

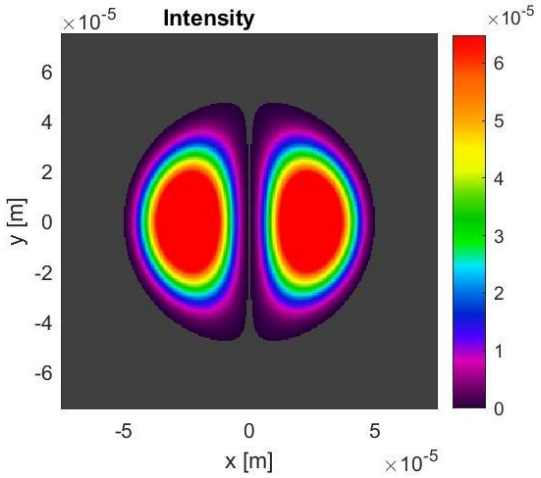

Figure 4. Intensity of the input field for the LP11 mode, without aberration

For the same core diameter, wavelength, and numerical aperture, supposing a fiber length of L = 10 cm, a defocus aberration with known strength b = 0.5 has been added and the field propagated. The output is depicted in Figure 5.

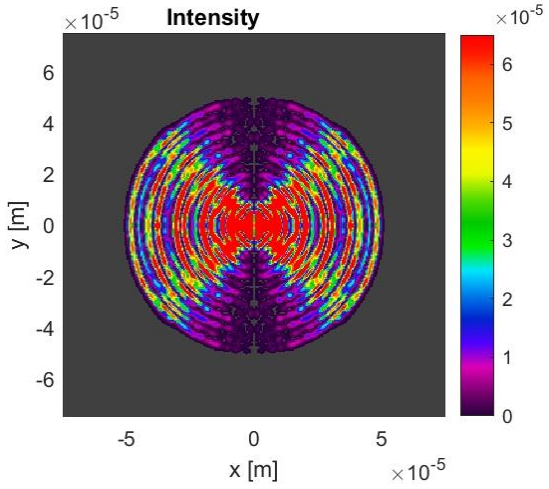

Figure 5. Intensity of the output field with defocus aberration and fiber length L = 10 cm

In the next steps, the features listed at the beginning of this Section were changed to study the corresponding effects.
It is worth underlying that the NA and core diameter values were specifically selected to meet the criteria classifying the fiber as multimode, through the V parameter:

$$V = \frac{2\pi a}{\lambda}\sqrt{NA} > 2.4$$

Differently from the previous figure, changing the length of the fiber brings a slightly different output pattern, that however maintains some features. In Figure 6, we presented the results showcasing the output of fibers with varying lengths when exposed to the same aberrated input field and fiber geometry, leaving the NA=0.24.

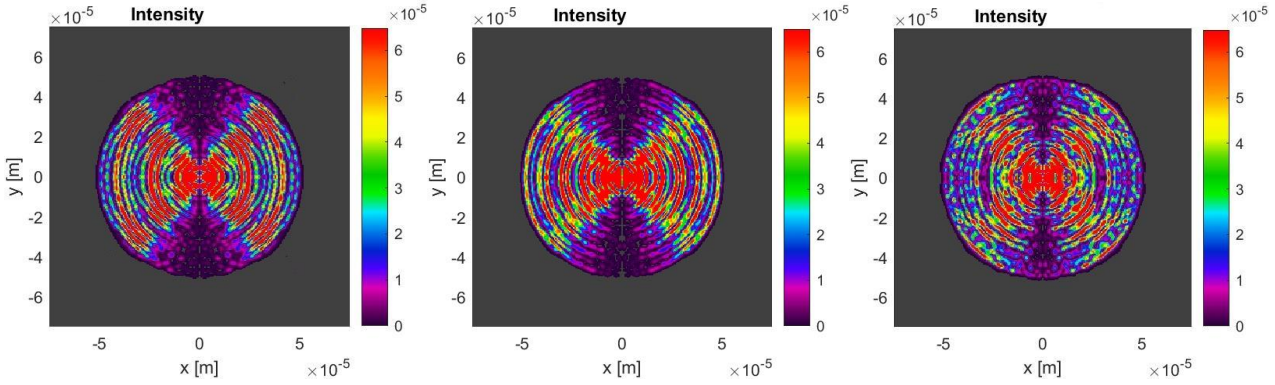

Figure 6. Intensity at the fiber output for an input defocus aberration. The fiber has 100 um of core diameter. The fiber length was changed to see the effect on the pattern. From the left: L = 5 cm, L = 10 cm, L = 20 cm

The same experiment was repeated by varying the fiber core: first by halving it to a value of 50 µm (Figure 7), and then doubling it to a value of a = 200 µm (Figure 8). Although the output pattern undergoes modifications, it is still possible to observe common features among the studied cases. However, it is also important to mention that for higher values, we cannot declare the same. For L = 40 cm, in fact, it was demonstrated that the output shows a totally different pattern, so it could be considered one of the critical parameters for the study.

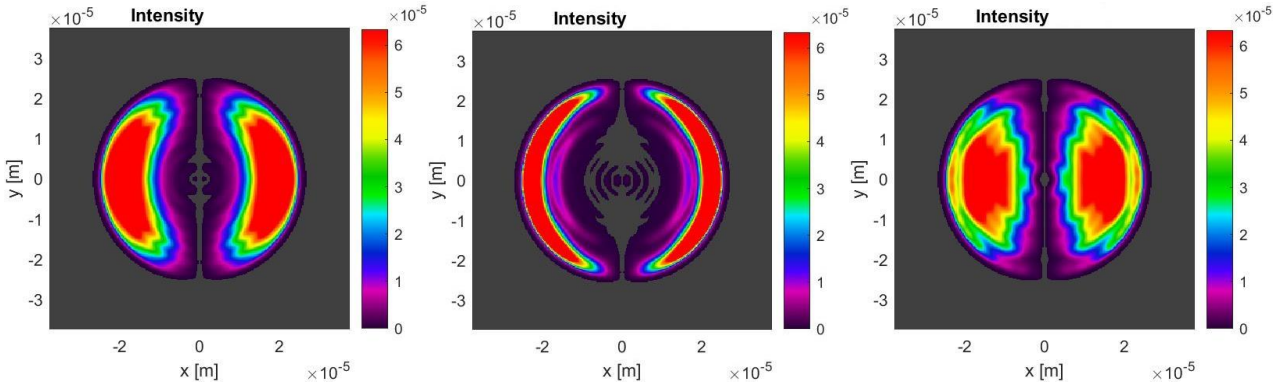

Figure 7. Intensity at the fiber output for an input defocus aberration. The fiber has 50 um of core diameter. The fiber length was changed to see the effect on the pattern. From the left: L = 5 cm, L = 10 cm, L = 20 cm

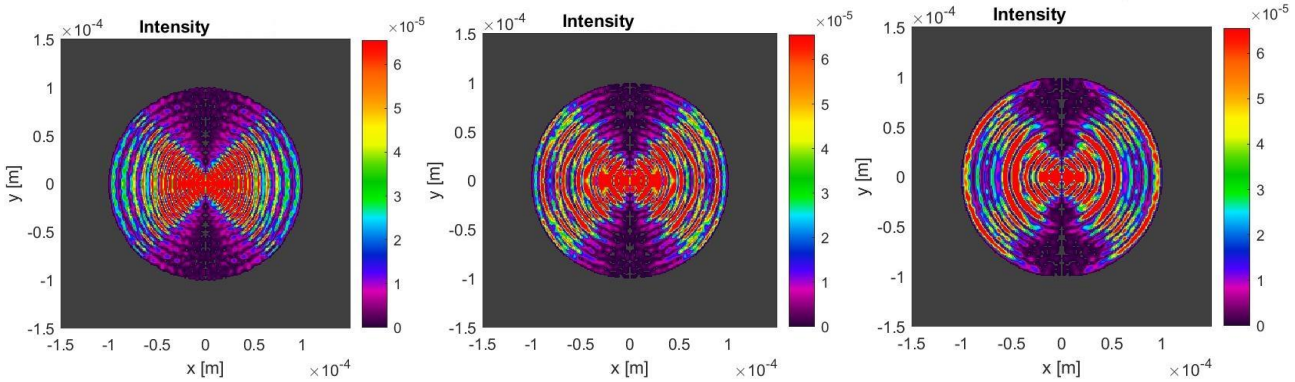

Figure 8. Intensity at the fiber output for an input defocus aberration. The fiber has 200 um of core diameter. The fiber length was changed to see the effect on the pattern. From the left: L = 5 cm, L = 10 cm, L = 20 cm

Subsequently, further simulations were conducted to assess the impact of numerical aperture variation. In this case, the length is fixed to L = 10 cm, and we choose fibers with core diameters respectively equal to a = 100 um and a = 200 um. In Figure 9, the outputs for a = 100 um are reported. Even for different values, the NA itself does not seem to heavily alter the output pattern, but a further investigation on the variations related to the index profile modifications must be carried out.

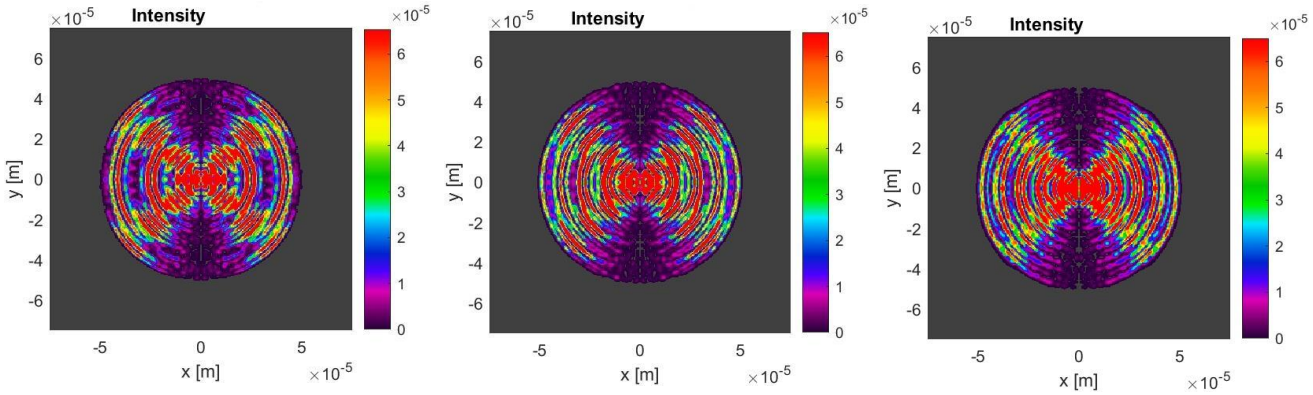

Figure 9. Intensity at the fiber output for an input defocus aberration. The fiber has 100 um of core diameter. The NA was changed to see the effect on the pattern. From the left: NA = 0.24 cm, NA = 0.29 cm, NA = 0.34

With respect to the core diameter, previous images clearly demonstrate that halving or doubling its size led to a modification in the pattern. The probable cause lies in the correlation between the increase in core diameter and a corresponding rise in the number of excited modes within the fiber. This phenomenon induces interference among the modes, ultimately yielding a more intricate output. For what concerns the modification of wavelength range, simulations guaranteed just one λ at a time, which for real applications seems not to be the best choice. This is something that will be better explored with an optical setup and different light sources.
Besides the fiber geometry, another fundamental aspect to consider is the effect of different aberrations on the input.
The previous images belong to cases where just defocus was applied to the initial wavefront. An exploration into the superposition of other aberrations has been investigated and here reported (Figure 10).
We compare and calculate the level of similarity between the aberration-free LP11 mode fiber input with the output obtained by superimposing to the initial phase different Zernike polynomials. The values of the coefficient *b*, which quantifies the magnitude of the aberration, were chosen as b=0.5 and b=1.5.
Notably, for horizontal coma and vertical coma, especially with higher coefficients, we gradually have a lower level of similarity with respect to the other. Whereas, as the spatial frequency increases, the effect of propagation through the fiber does not show many undesirable effects, guaranteeing a high value of similarity.

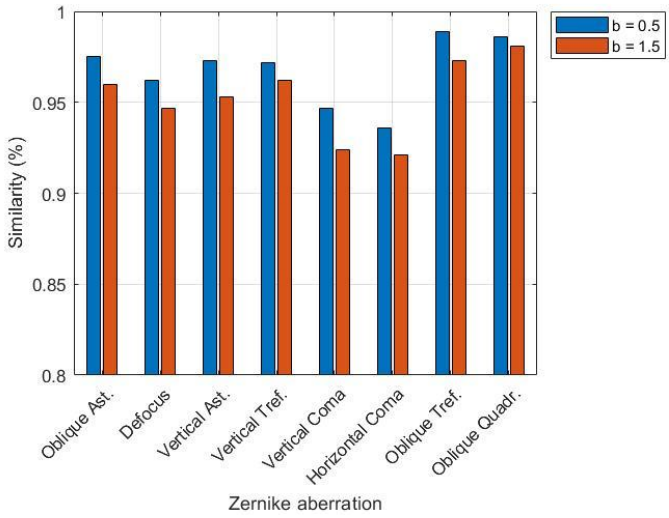

Figure 10. Level of similarity between aberrated-free input field and Zernike aberrated ones at the fiber output

In this last simulation results, instead, we explore the outcomes obtained by overlaying five different Zernike aberrations onto the initial input field. The length is fixed to L = 10 cm and the NA = 0.29. The results are reported in Figure 11.

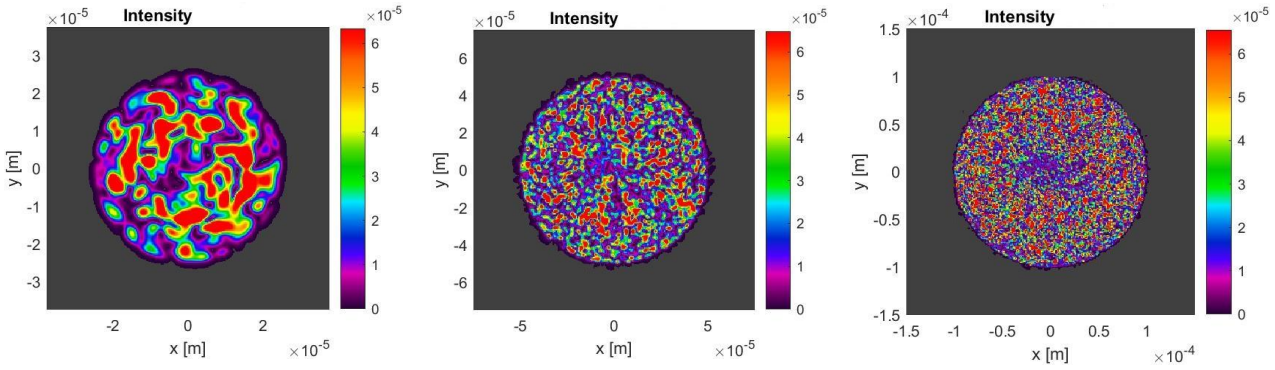

Figure 11. Intensity at the fiber output with 5 Zernike aberrations superposition for different fiber core diameters. From the left: a = 50 um, a = 100 um, a = 200 um

It was observed that, for all three diameters, an increase in coefficient *b* results in the formation of intricate spackles, even with a significant reduction in the fiber length, i.e., with $L < 5$ cm.
Additionally, it is evident that a larger diameter leads to a greater number of excited modes, resulting in a more complex output.
Only with a fine-tuning of the NN and an ingenious approach to the critical parameters, one can exploit the advantages for our specific applications.

4. FUTURE WORK

Simulations have demonstrated that by varying specific fiber parameters, various critical aspects can be explored. Therefore the first step of the future work will be to set up a testbench as shown in Figure 12, to replicate the simulated experiments, validate commonalities, and introduce additional factors crucial for the neural network's advancement.

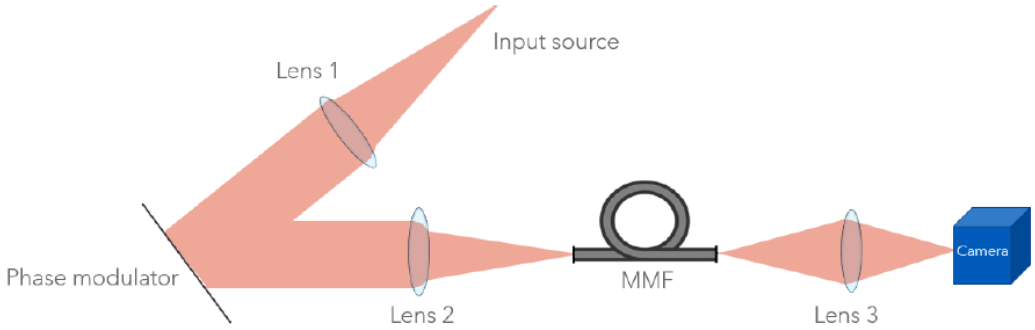

Figure 12. Schematic representation of the optical test bench for laboratory experiments

In the scheme, the phase modulator, controlled by software, will inject a known distortion so that one has full control on the input, while a camera is used to acquire data of the propagated wavefront at the fiber output. This stage is fundamental to create a suitable set of images, as done in simulations.
The experiments necessitate maintaining the fiber in a controlled environment to allow a proper initial calibration.
For what concern the NN, we foresee to use a Convolutional Neural Network (CNN). Moreover, it will be necessary to characterize some aspects such as the size of input/output images, the types of filters to be used, the parameters and attributes of interest for the training phase as well as the size of the training and test sets for the validation. A user-friendly and easy program such as Scikit-Learn in Python will be used for basic operations of clustering and classification. This will be helpful to understand the discriminant factors of the input images. Then, more specialized software applications based on ML Python packages such as Tensorflow/Keras will be employed. The network architecture, at least in a preliminary stage, will be comparable to the models in literature (VGG, U-Net, Inception, etc.), then one will adapt this first approach to the specific case, changing the number of convolutional layers, epochs, and batches, while finding well-suited activations function and optimization algorithms. This step will be essential because it leads to better evaluating the training and pattern recognition time and accuracy, which is of crucial importance in real-time applications.

5. CONCLUSIONS

We presented a new proposal for a feasibility study aimed at the investigation of photonic waveguides as probes for focal plane wavefront sensing with the contribution of ML. This allows us to overcome the reconstruction complexity of the transmitted wavefront in highly scattering media. MMFs, in particular, have gained exponential interest due to their versatility, transmission capacity, and high resolution. We are confident that the combination of such photonics devices with the potentialities of ML in real-time applications will open new doors for the use of these emerging technologies in Adaptive Optics for highly performed astronomical instrumentation.

REFERENCES

[1] Azadeh, M., “Fiber Optic Communications: A Review”, Fiber Optics Engineering, Optical Networks (Springer US, 2009)

[2] Richardson, D. J., Fini M., Nelson L. E., “Space-division multiplexing in optical fibers”, Nature Photonics 7, 354-362, 2013

[3] Yin, S. and Ruffin, P., “Fiber optic Sensors”, Wiley Encyclopedia of Biomedical Engineering, American Cancer Society, 2006

[4] Thévenaz, L. and Soto, M. A., “Novel Concepts and Recent Progress in Distributed Optica Fiber Sensing”, Optical Fiber Communication Conference, OSA, 2016

[5] Katzir, A., “Lasers and Optical Fibers in Medicine”, Elsevier, 2012

[6] Elahi, S. F., Wang T. D., “Future and advances in endoscopy”, J. Biophoton 4, 471-481, 2011

[7] Arribas, S., Mediavilla E. and Watson F., “The astronomical uses of Optical Fibers”, Fiber Optics in Astronomy III, ASP Conference Series, Vol. 152, 1998

[8] Sauvage, JF., et al., “Calibration and precompensation of non-common path aberrations for extreme adaptive optics”, J Opt Soc Am. A Opt Image Sci Vis, 2007

[9] Pourrè, N., et al "Understand and correct for the low wind effect on the SPHERE and GRAVITY+ adaptive optics", Proc. SPIE 12185, Adaptive Optics Systems VIII, 2022

[10] Corrigan, M.K., Morris, T.J., Harris, R.J., “Demonstration of photonic lantern low order wavefront sensor using an adaptive optics testbed”, Adaptive Optics System VI Conf, 2018

[11] Norris, B.R.M., Wei, J., Betters, C.H., et al., "An all-photonic focal-plane wavefront sensor", Nat Commun 11, 5335, 2020

[12] Kakkava, E., “Wavefront shaping and deep learning in fiber endoscopy”, Thesis of Ecole Politechnique Fédérale de Lusanne, 2020

[13] Rahmani B., et al., “Multimode optical fiber transmission with deep learning”, Light: Science & Application, 2018

[14] Chai, J., Liu, W., Zhang, K., Lu, Y., et al., “Influence of aberrations on Modal Decomposition for LMA Fiber Laser System, Front. Physics, 2022

[15] Zheng, D., Li, Y., Chen, E., et al., “Free space to few-mode fiber coupling under atmospheric turbulence”, Optic Express, 2016

[16] Veettikazhy, M., Anders, K.H, Dominik, M., et al. , “BPM-Matlab: an open-source optical propagation simulation tool in MATLAB”, Optic Express, 2021